Nuclear Astrophysics
Lecture 2

Overview of lectures

1. A little stellar astronomy

2. A bit more on scattering theory

3. $^{12}C(\alpha,\gamma)^{16}O$, some discussion, new results
4. $^{40}Ca(\alpha,\gamma)^{44}Ti$

5. $\mathbf{^{7}Be(p,\gamma)^{8}B}$ experiment

6. $^{7}Be(p,p)^{7}Be$

7. Tactic

8. Radioactive beam experiments at TRIUMF

2nd lecture

Radiative capture

The transition matrix for radiative capture can be written as:

$$U^{\sigma LM} = \sqrt{\frac{T_{i\to f}^{\sigma LM}}{2J+1}}$$

The scattering matrix then contains three terms:

$$U^{\sigma LM} = \text{resonance term} + \text{hardsphere term} + \text{channel term}$$

The channel term is usually incorporated into the resonant term by making the reduced width amplitudes complex and energy dependent. Specializing to E2 capture:

$$U_{J_f}^{J_i} = -ie^{i(\omega_{J_i}-\phi_{J_i})} 2P_{J_i}^{1/2} k_\gamma^{5/2} [\sum_{\lambda\mu} \gamma_\lambda^{J_i} \gamma_{\mu\gamma J_f}^{J_i} A_{\lambda\mu}^{J_i} + \frac{3}{\sqrt{10}} \frac{M_N e}{\hbar k} N_f^{1/2} a^2 \ F_{J_i}(a) G_{J_i}(a)$$

$$i^{J_i+2-J_f} \theta_f^{J_f} (J_i 200 | J_f 0) J_2^{'}(J_i, J_f)]$$

hardsphere term

Radiative capture

Therein is:

M_N-nucleon mass

$$\gamma^{J_i}_{\mu\gamma J_f} = \frac{3}{\sqrt{10}} \frac{M_N e}{\hbar} N_f^{1/2} a^3 i^{J_i+2-J_f} \gamma^{J_i}_{\mu} (J_i 200 | J_f 0)[J_2''(J_i, J_f) + i \frac{F_{J_i}(a) G_{J_i}}{F_{J_i}^2(a) + G_{J_i}^2(a)} J_2'(J_i, J_f)]$$

The energy dependent reduced width amplitude. Therein are overlap functions between Whittacker functions and Coulomb functions:

$$J_L'(\ell, \ell'_f) = \frac{1}{a^{L+1}} \int_a^\infty dr r^L \frac{W_{\ell'_f}(r)}{W_{\ell'_f}(a)} \left[\frac{F_\ell(r)}{F_\ell(a)} - \frac{G_\ell(r)}{G_\ell(a)} \right]$$

$$J_L''(\ell, \ell'_f) = \frac{1}{a^{L+1}} \int_a^\infty dr r^L \frac{W_{\ell'_f}(r)}{W_{\ell'_f}(a)} \frac{F_\ell(a) F_\ell(r) + G_\ell(a) G_\ell(r)}{F_\ell^2(a) + G_\ell^2(a)}$$

with the normalization:

$$N_f^{-1} = 1 + \frac{2(\theta_f^{J_f})}{a} \int_a^\infty dr \left[\frac{W_{J_f}(r)}{W_{J_f}(a)} \right]^2$$

Overlap integrals between external and internal wavefunctions;

Space for theory

Radiative capture

In single channel approximation is:

$$\sum_{\lambda\mu}\gamma_{\lambda}^{J_i}\gamma_{\mu\gamma J_f}^{J_i} A_{\lambda\mu}^{J_i} = \frac{\sum_{\lambda}\dfrac{\gamma_{\lambda}^{J_i}\gamma_{\mu\gamma J_f}^{J_i}}{E_{\lambda}^{J_i}-E}}{1-(S_{J_i}-B_{J_i}+iP_{J_i})\sum_{\lambda}\dfrac{\gamma_{\lambda}^{J_i}}{E_{\lambda}^{J_i}-E}}$$

i.e., containing the *R*-matrix.

The direct E1 capture is heavily suppressed, as the cross section is multiplied with the effective charge:

$$\bar{e}_L = \mu\left[\frac{Z_1}{M_1}+(-)^L\frac{Z_2}{M_2}\right]e$$

So called data
Ground State Transition Multipoles (E2)

As phaseshifts are known from elastic scattering, the ratio $\frac{\sigma(E_2)}{\sigma(E_1)}$ can be derived from these angular distributions in principle. From this usually separate cross sections σ_{E1} and σ_{E2} can be derived. However, this leaves their respective errors coupled and unfortunately frequently the principal value as well.

Some E2 data from literature.

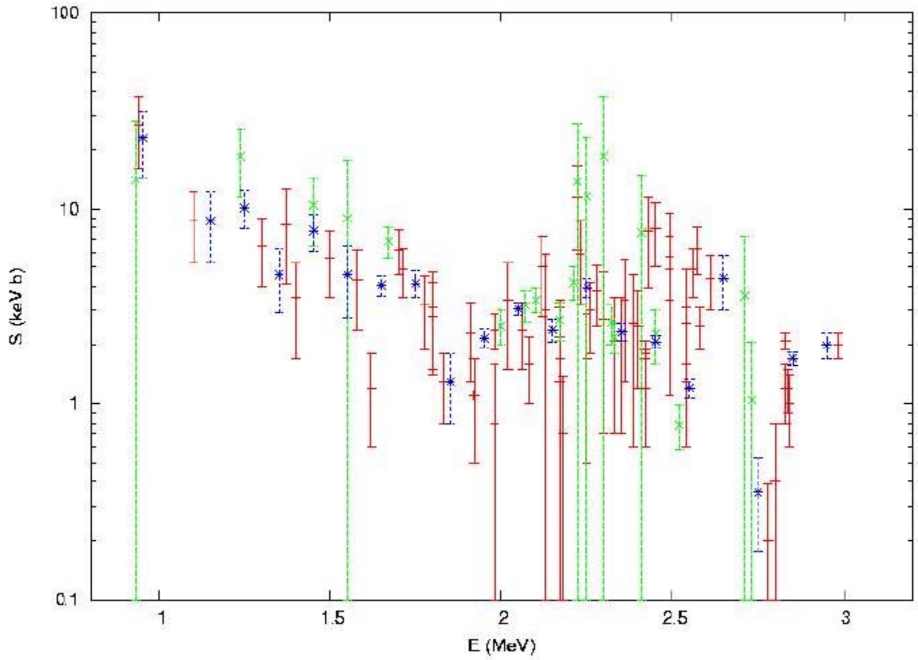

Unfortunately angular distributions are rarely published.

^{16}N spectrum-Input to fit

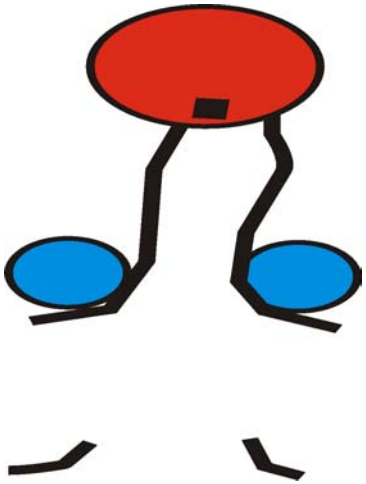

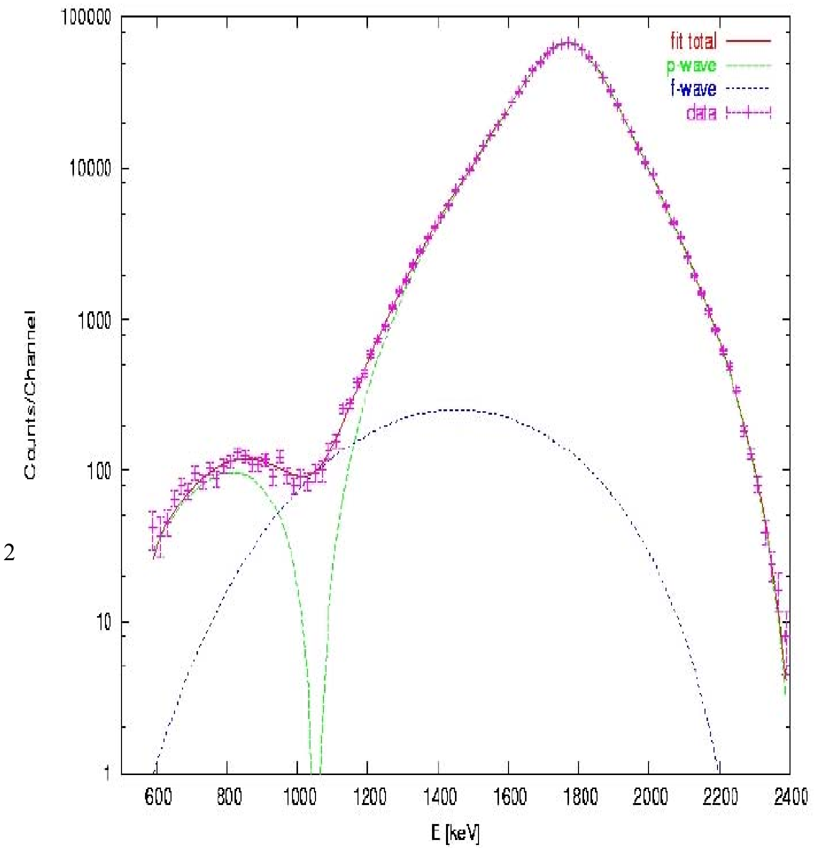

$$W_\alpha = f_\beta(E)\sum_{\ell=1,3} P_\ell(E,a_\ell)\left|\frac{\displaystyle\sum_{\lambda=1}^{q_\ell}\frac{A_{\lambda\ell}}{E_{\lambda\ell}-E}}{1-[S_\ell(E,a_\ell)-B_\ell+iP_\ell(E,a_\ell)]R_\ell(E)}\right|^2$$

RFQ and DTL

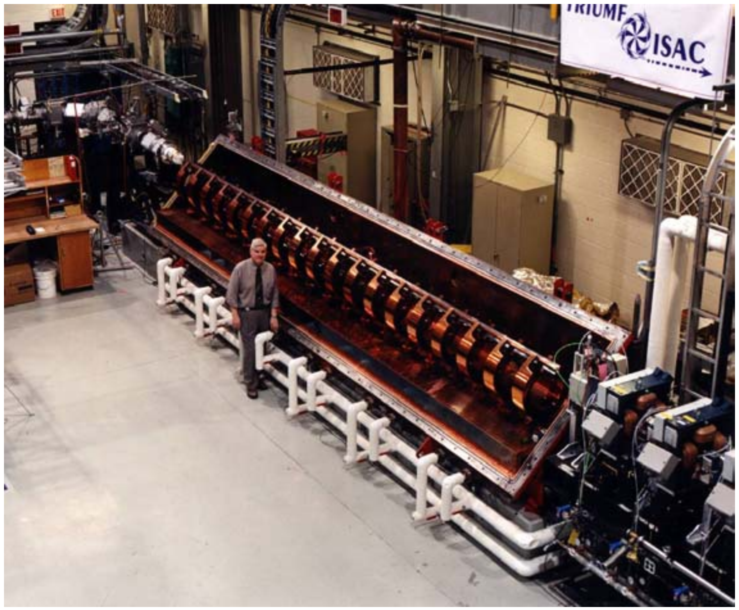

RFQ: 0.02→0.15 MeV/u

DTL tanks 0.15→1.5 MeV/u

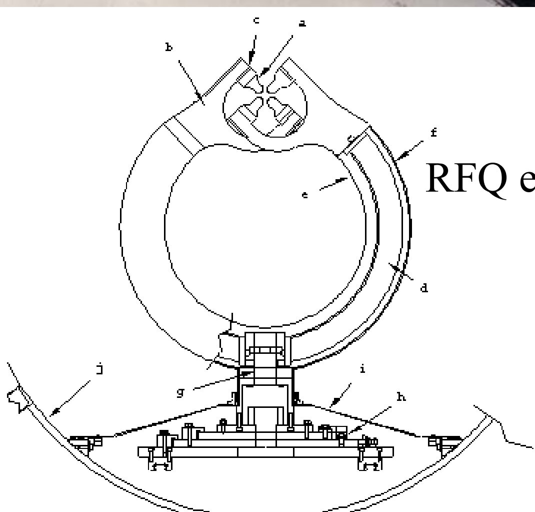

RFQ element

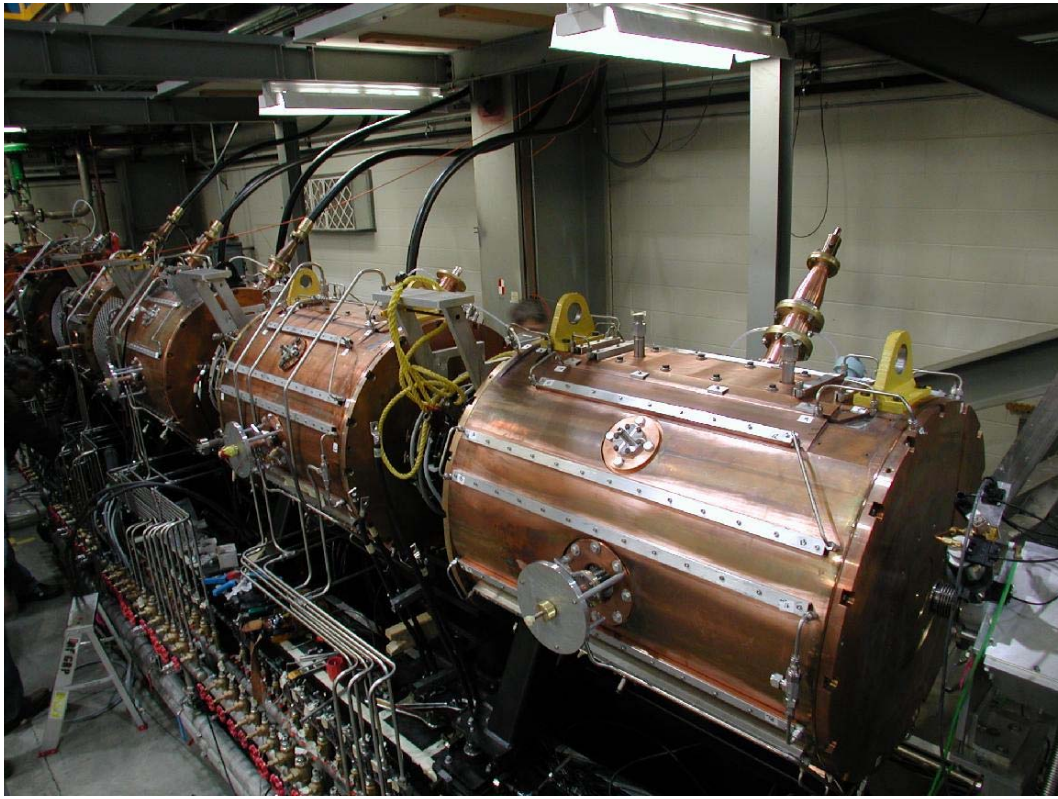

Recoil separators

In radiative capture reactions mostly γ-rays have been detected. However, there are problems with background, both natural and beam induced, and often with low efficiencies.

The simultaneous detection of recoil particles, i.e. the reaction product and γ-rays provides for often background free and highly efficient detection. (Backgrounds may result from random coincidences with leaky beam.)

Recoil particle and beam have essentially the same momentum. Therefore electric fields are required for separation of beam and recoils. The power of a separator can be judged by the electric field strength x field length.

Separating power typically has to be traded against recoil acceptance.

Detectors for direct measurements

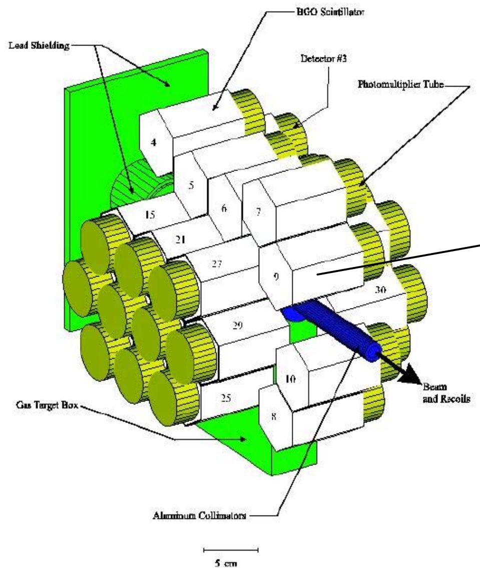

BGO array

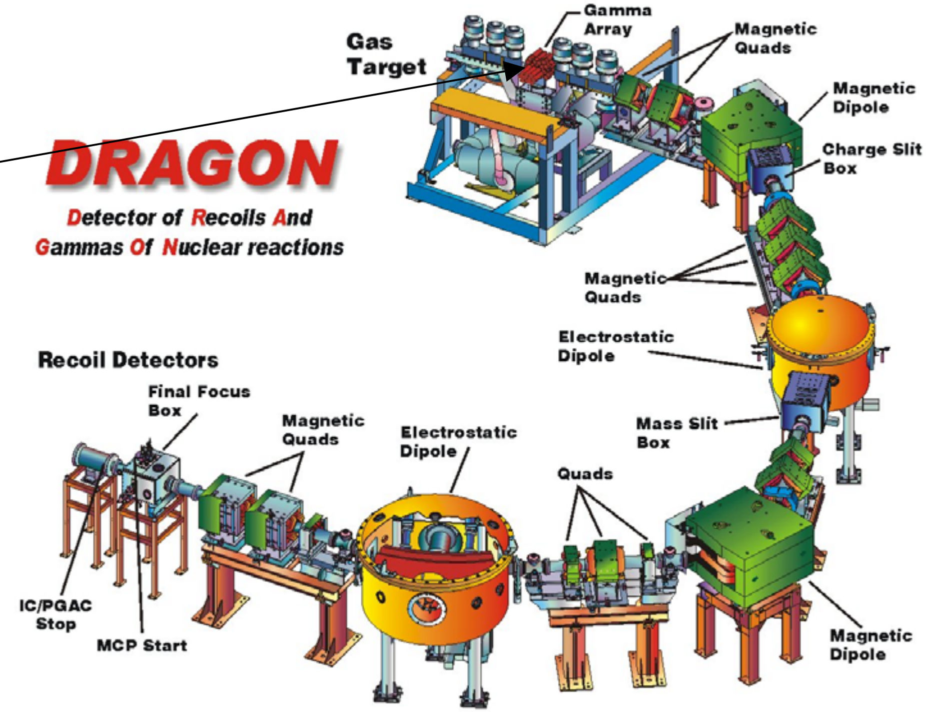

DRAGON

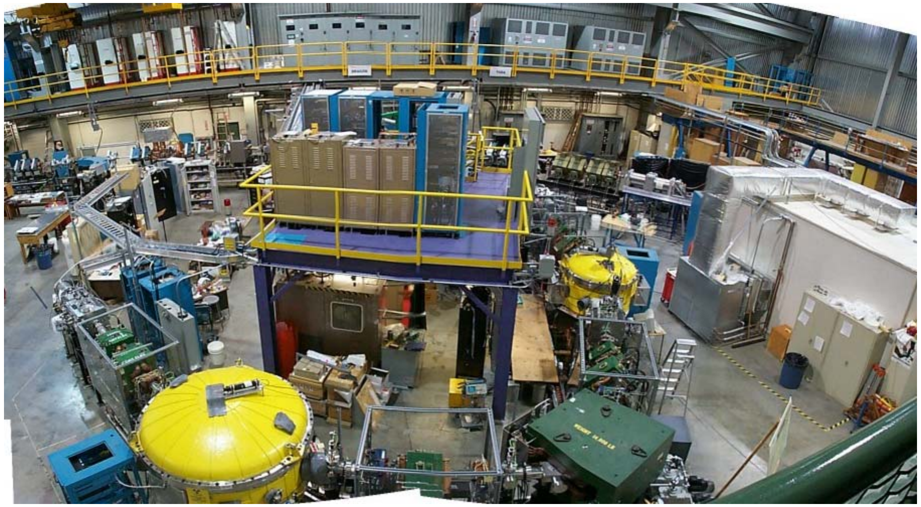

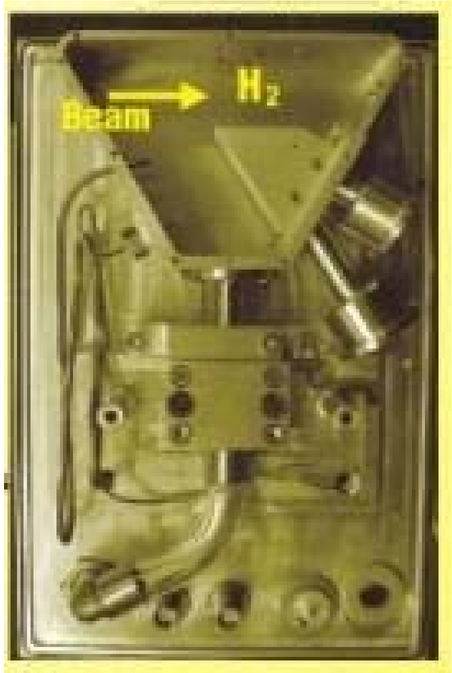

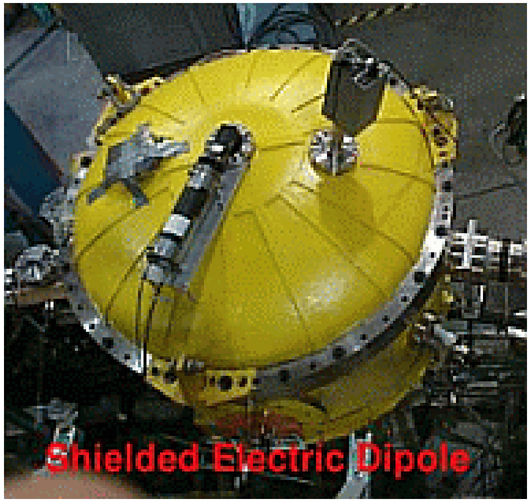

Electrostatic
bender

Target

Recoil signal in a silicon detector: DSSSD

Strip division hits

alpha-source

Recoil peak

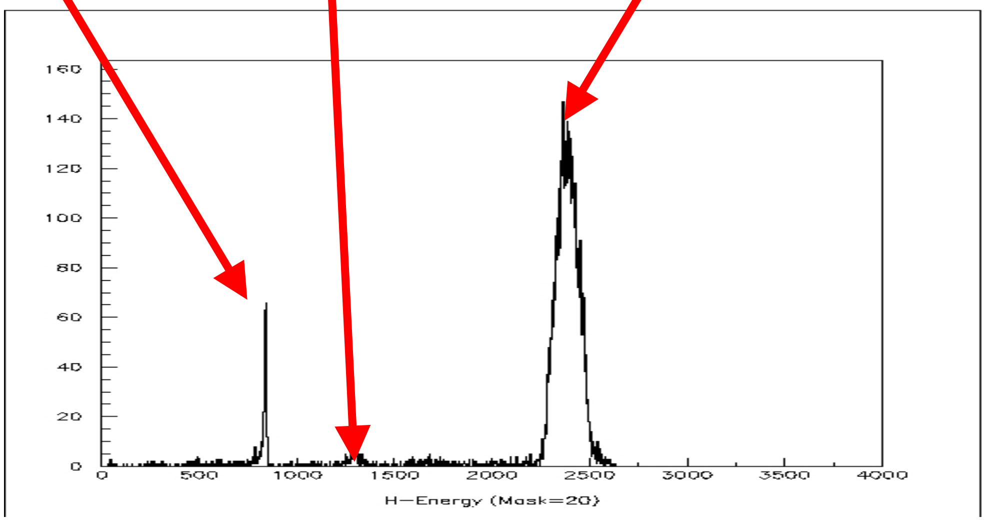

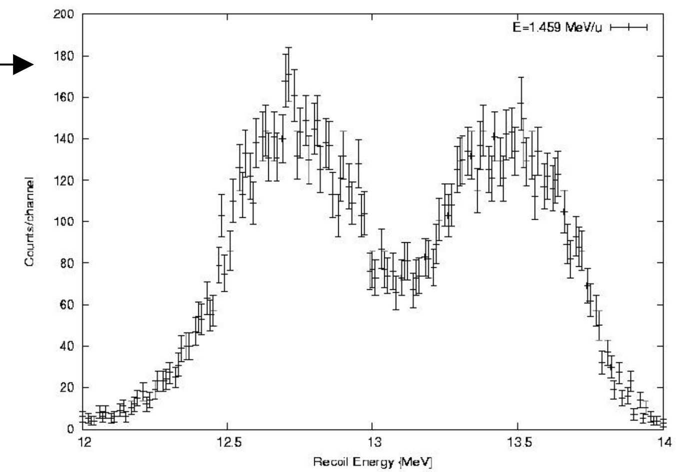

2^+ resonance

In upper 1^- resonance

Pretty much all the ground state transition data

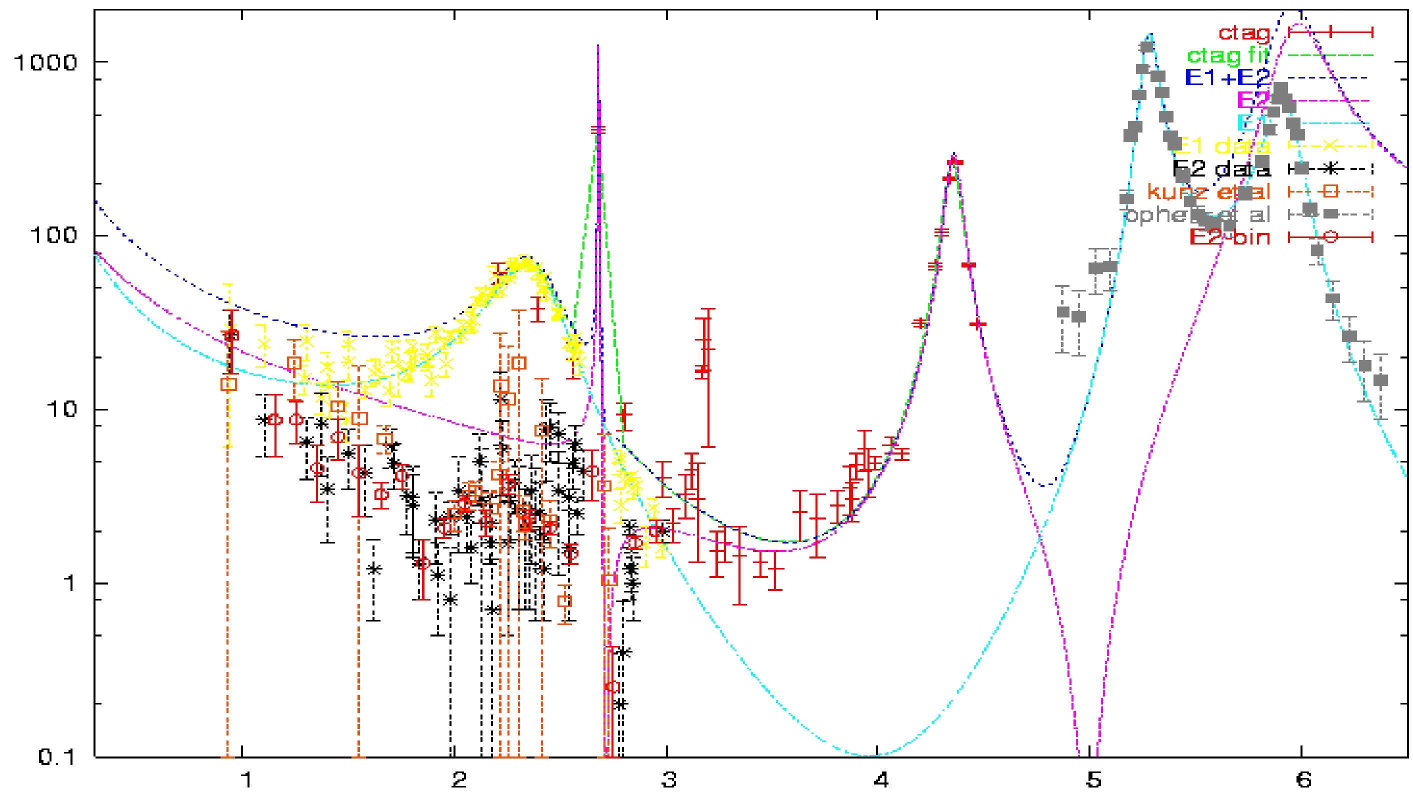

The S_{E2} interference sign

The interference sign between the direct capture part of the E2 ground state transition and the tail of the 6.9 MeV subthreshold resonance is unknown.

The low energy data make a destructive interference more likely while data above the 4^+ resonance seem to favour a constructive one.

The result for 300 keV is then: $S_{E2}(300)$=55 keV b or SE2(300)=90 keV b.

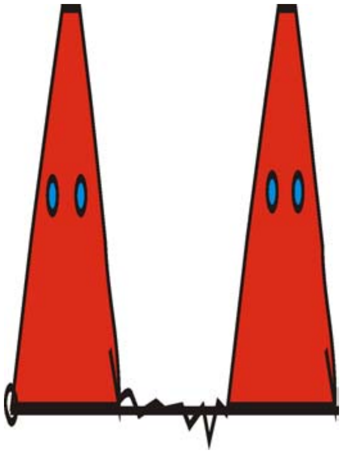

Cascade transitions

Possible cascades into the 6.0 (0^+), 6.1(3^-), 6.9(2^+) and 7.1(1^-) MeV states.

6.0: observed at DRAGON, reported below

6.13 Not observed, except for narrow 4^+ resonance.

6.9 observed over rather wide range

7.1 observed in broad 1^- resonance

S-factor prediction for 6.9 MeV cascade

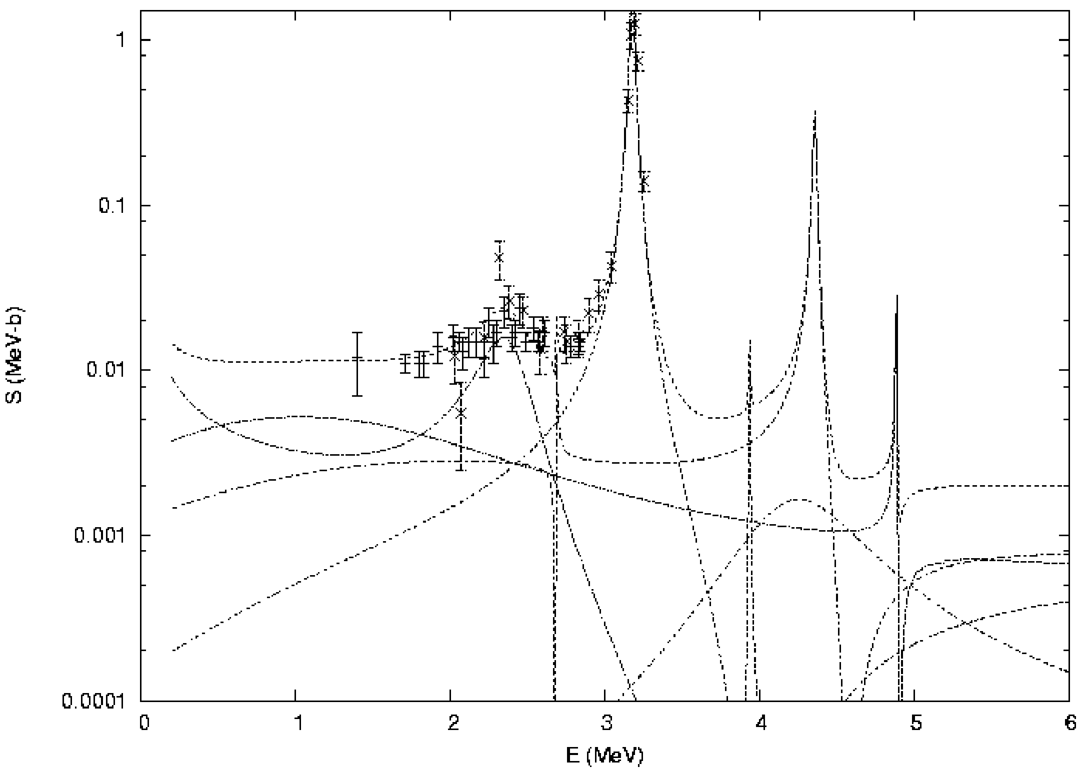

Observation of γ-decays

γ -ray spectrum at 0.945 MeV/u and GEANT3 fit to spectrum.

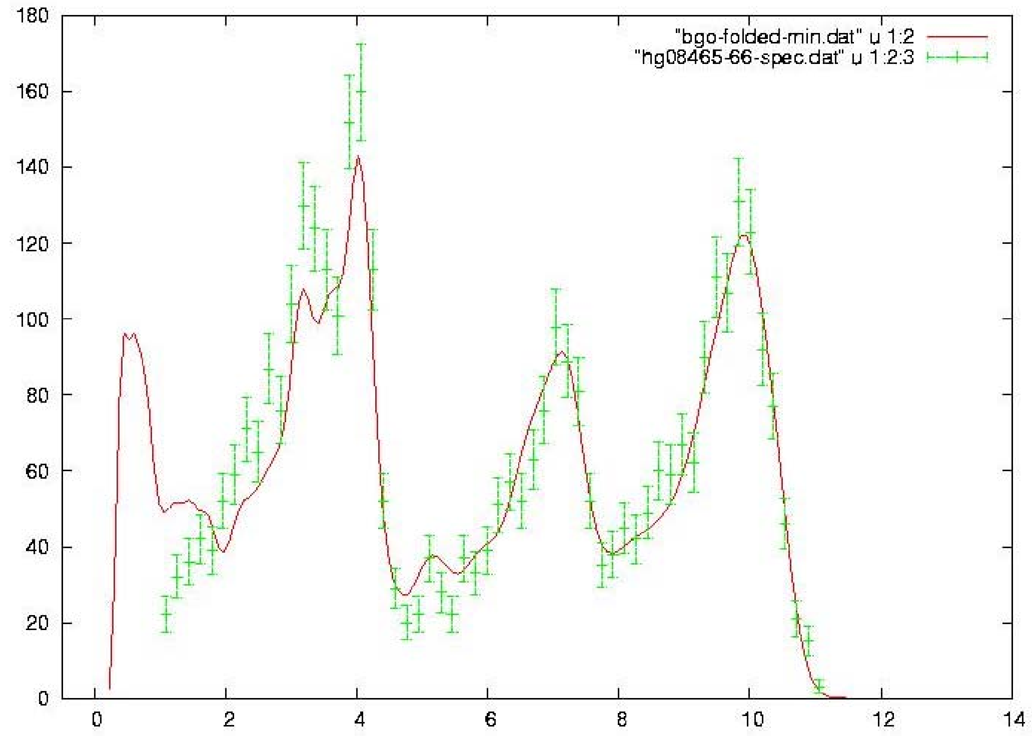

E→6.0 branching ratio

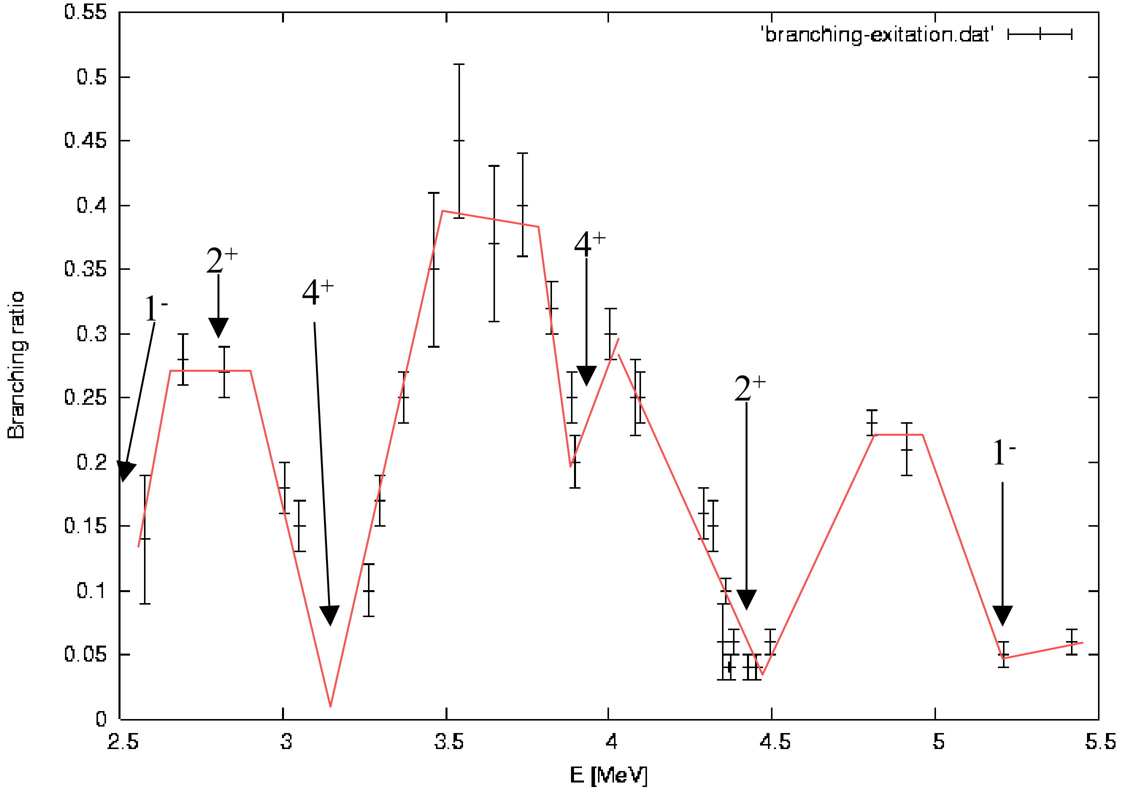

Error budget for E→6.0 measurement

TABLE II: Error budget for this experiment.

error cause	value
DRAGON acceptance/mistuning	+5%, -10%
angular distributions	5%
number of target atoms	10%
branching ratio	15%
charge state fraction ^{12}C	5%
charge state fraction ^{16}O	5%
beam current integration	3%
BGO array efficiency	5%
DSSSD efficiency	1%
Total	+20%, -18%

Total cross section measurement at ERNA

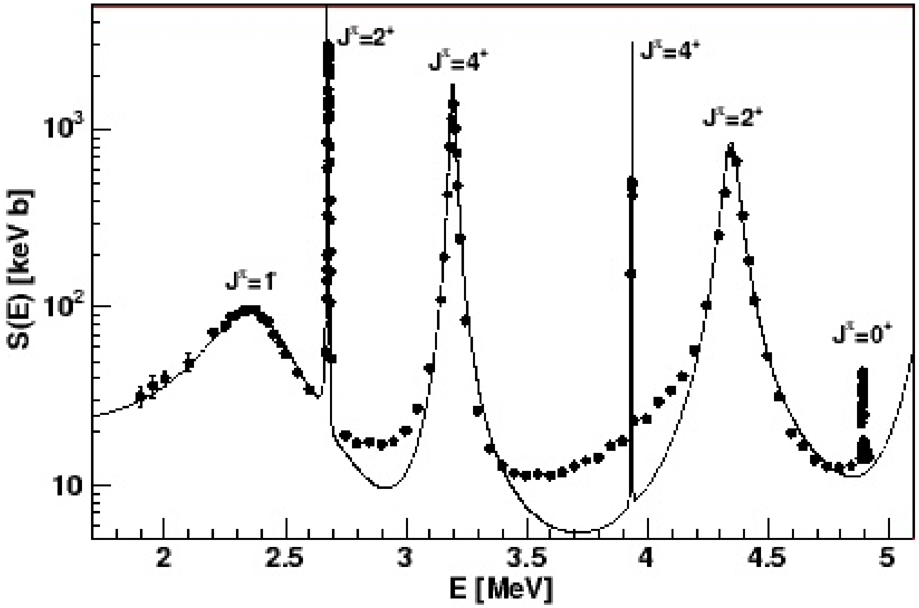

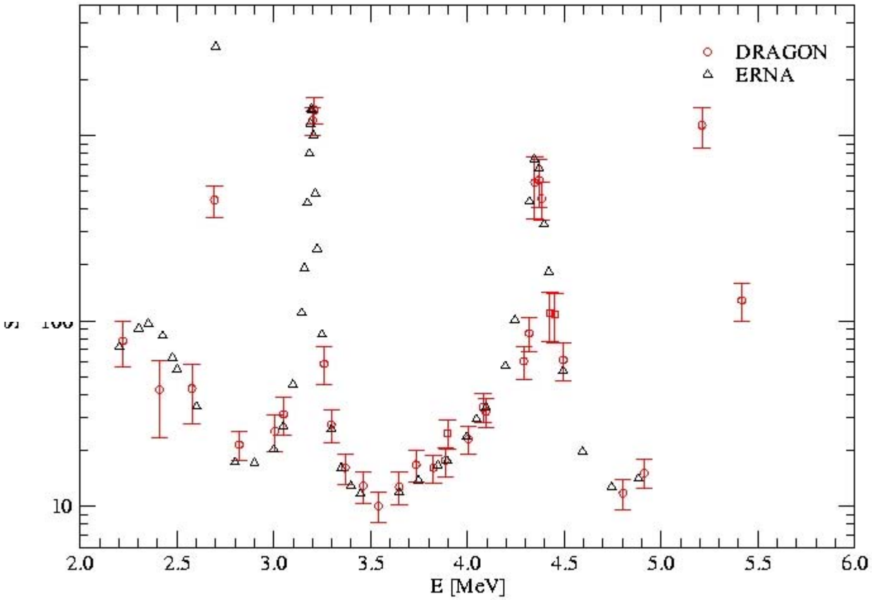

S-factor for the E→6.0 MeV cascade

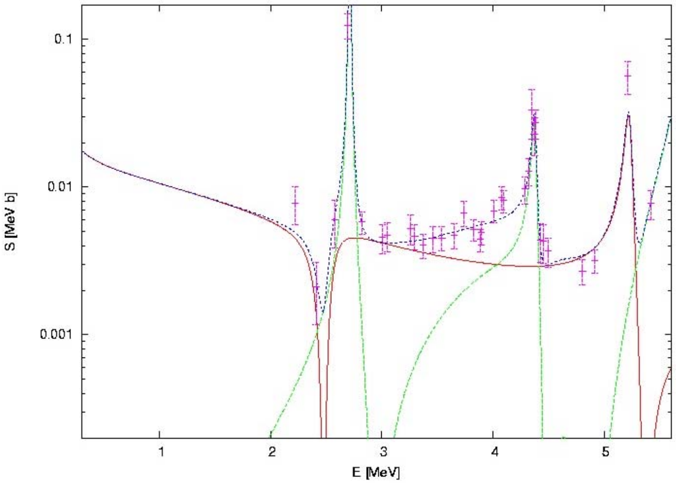

Negative θ_f solution: 18±9 keV b

Averaged result: 22±13 keV b

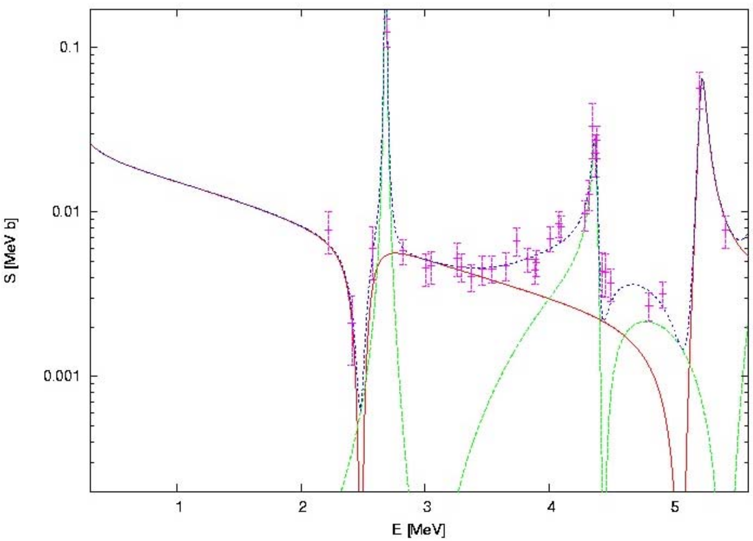

Positive θ_f solution: 26±9 keV b

Parameter scans and S-factor

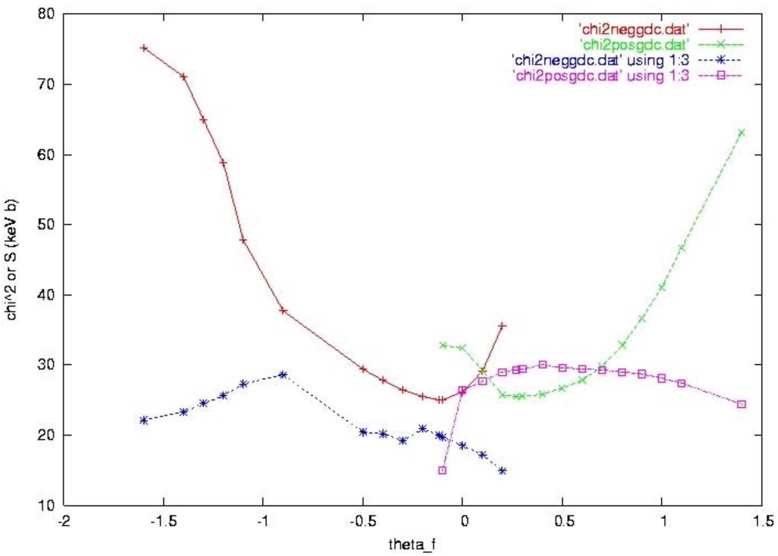

E2 direct capture strength

solution switches

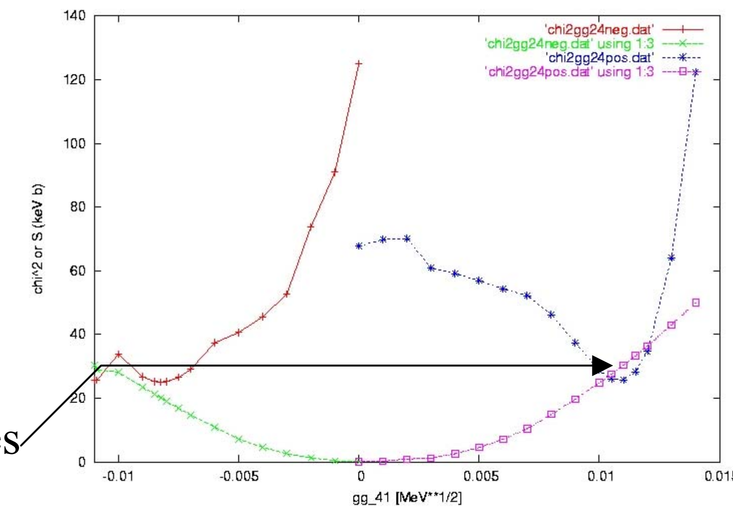

E1 background state strength

^{40}Ca(α,γ)^{44}Ti at DRAGON: Overview

- ^{44}Ti production in α-rich freeze out. ^{44}Ti (60 a) observed in γ-ray astronomy. Direct gamma and AMS results contradict.

- Micro-wave source:

  stable beam, 0.5% ^{40}Ar contamination, current up to 20 enA on target,
  ~ 5 x 10^{15} ^{40}Ca on target

- Very good beam tune:

  90% transmission trough DTL, small spot size, buncher on

- >50 energy changes

  Procedure involved interaction between operator and experimenter

- Energy range covered so far: 1140 – 840 keV/u

- Charge State Booster: SiN foils last >600 nA h

Beam spot on Target

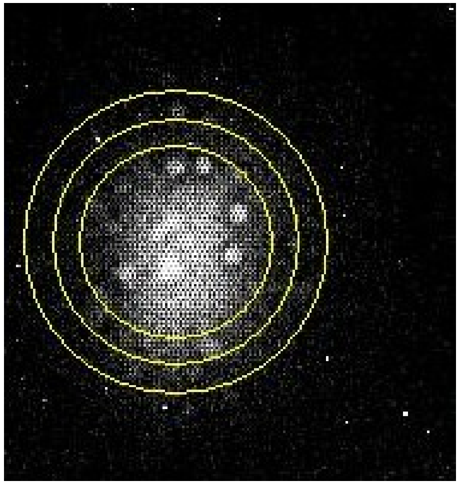

August 05

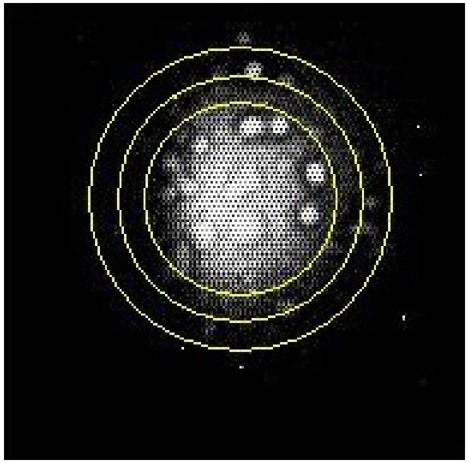

September 05

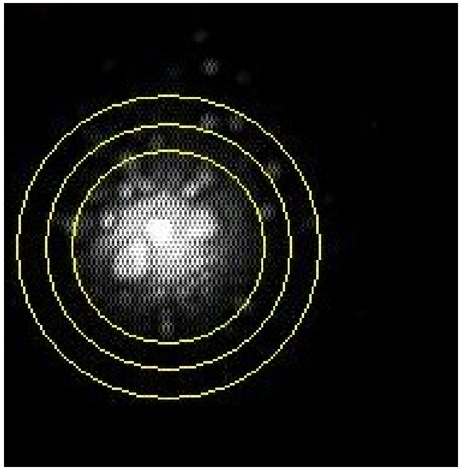

November 05

^{44}Ti identification

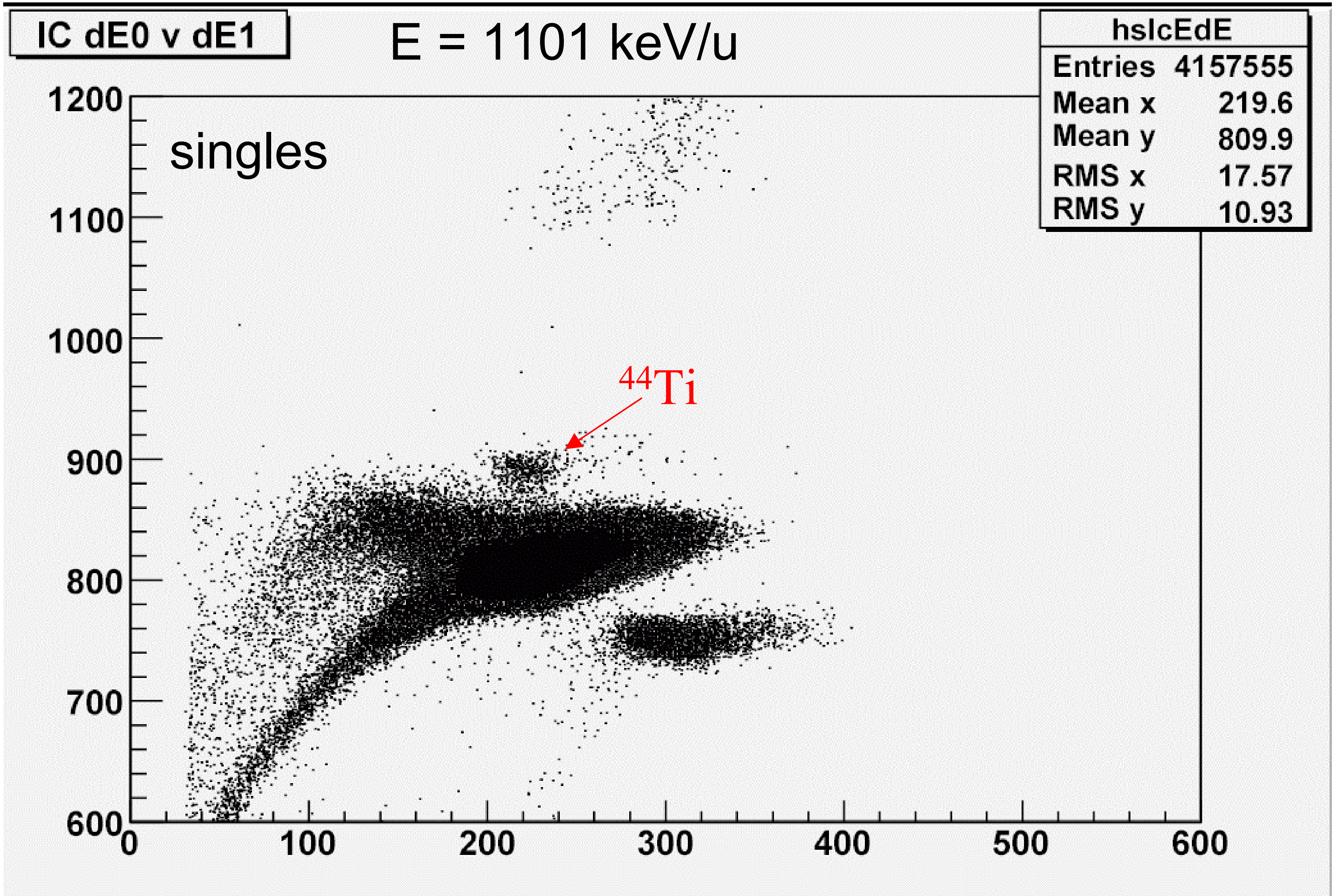

^{44}Ti identification

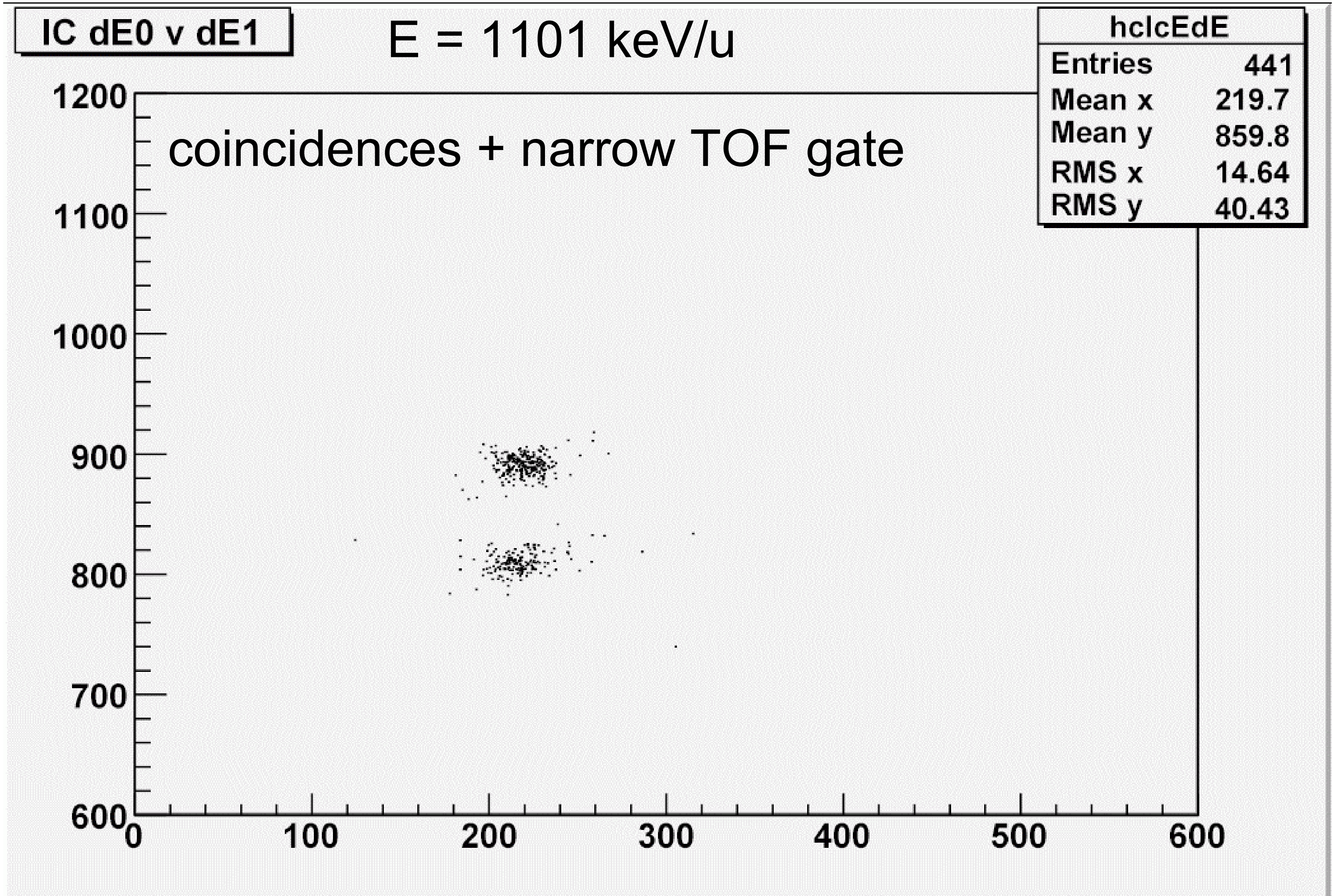

Excitation function

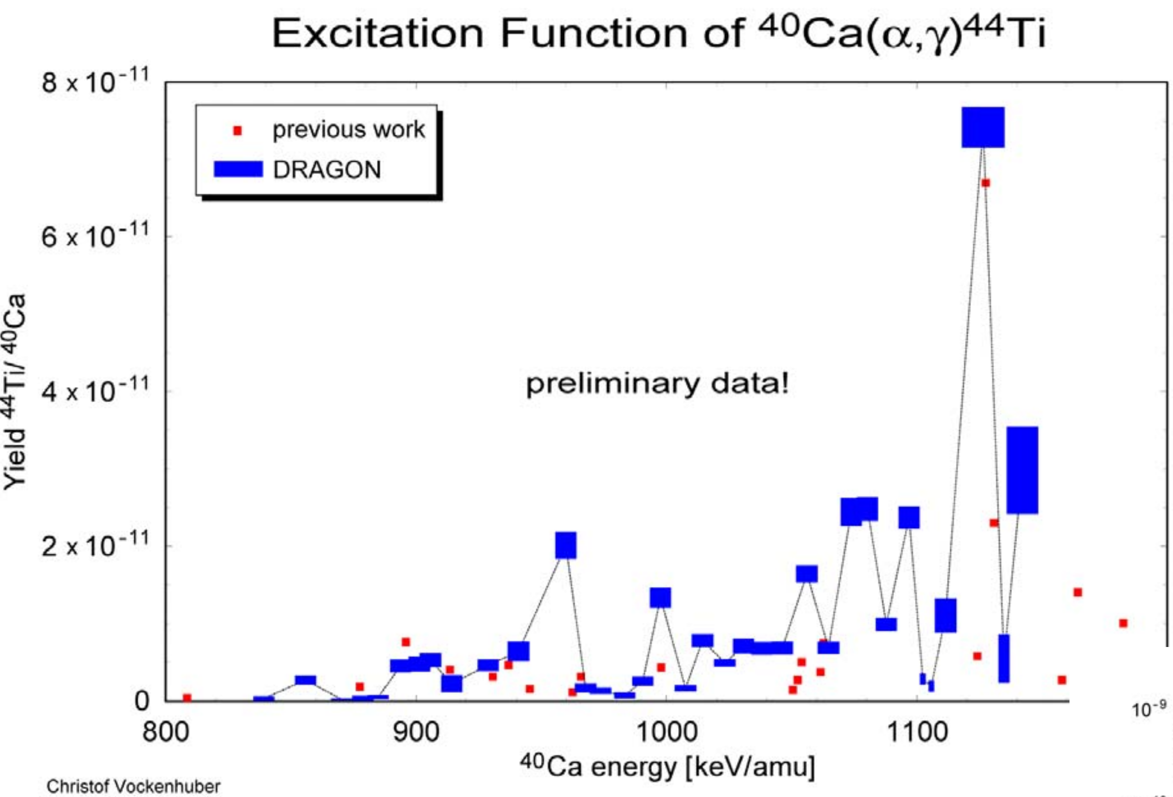

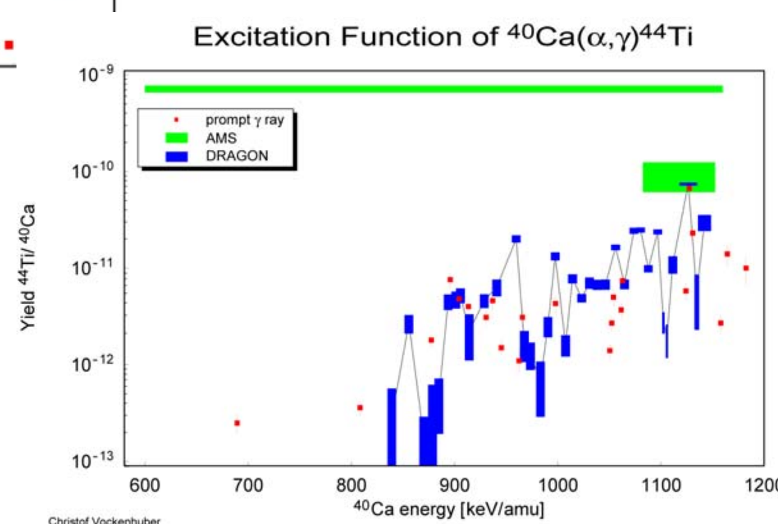

Preliminary result: many small resonances seem to be overlooked in direct measurements.

Hydrogen Burning

- Most of their lives, stars burn hydrogen, the most abundant and simplest element. There are two principle reaction chains: The pp process and the CNO cycle. For the sun, the pp chain is most important.

$$p + p \rightarrow d + e^{+} + \nu_e$$

$$d + p \rightarrow {}^{3}He + \gamma$$

$${}^{3}He + {}^{3}He \rightarrow {}^{4}He + 2p$$

$${}^{3}He + \alpha \rightarrow {}^{7}Be + \gamma$$

$${}^{7}Be + e^{-} \rightarrow {}^{7}Li + \nu_e$$

$${}^{7}Li + p \rightarrow 2\alpha$$

$${}^{7}Be + p \rightarrow {}^{8}B + \gamma$$

$${}^{8}B \rightarrow {}^{8}Be + e^{+} + \nu_e$$

$$\downarrow 2\alpha$$

Up to 300 mCi

A ^{7}Be target

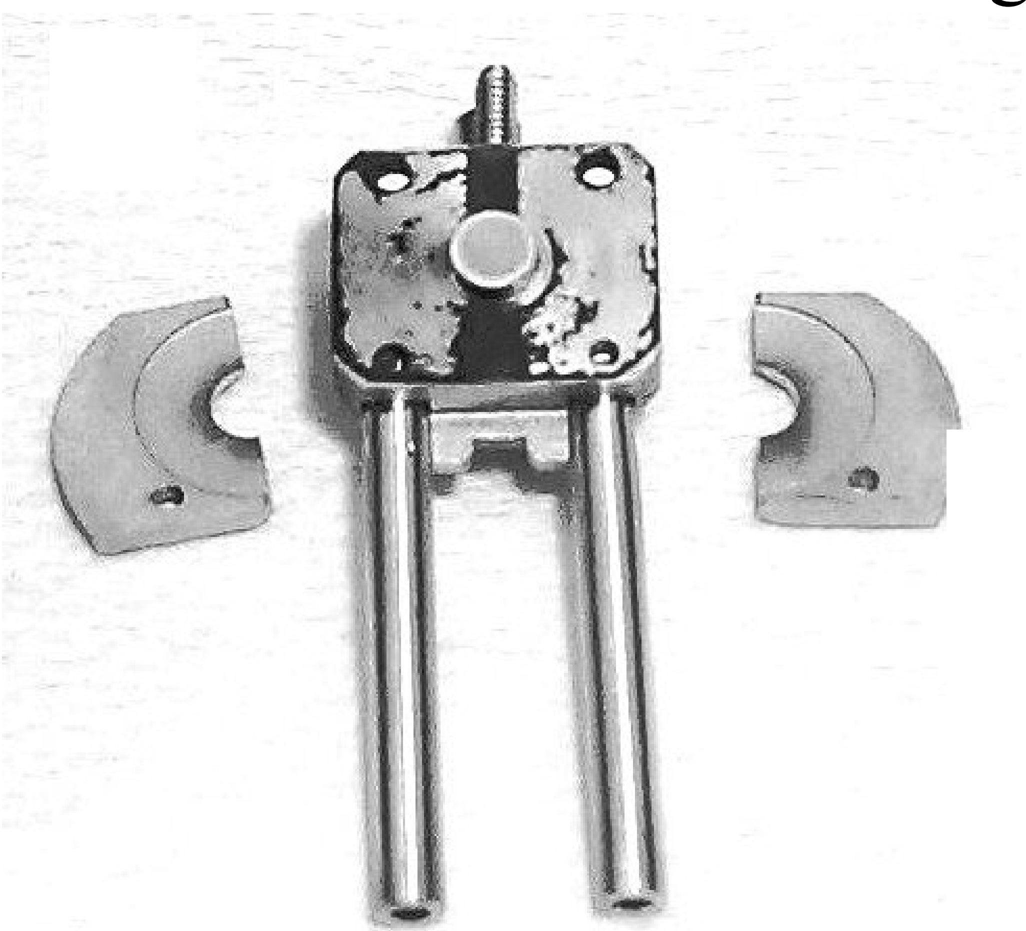

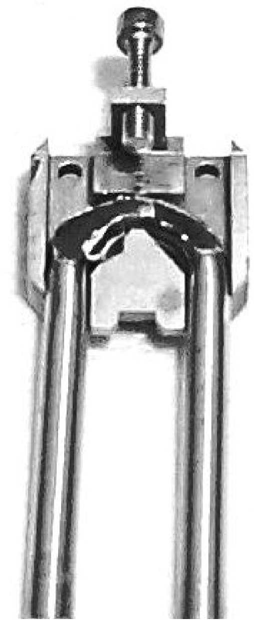

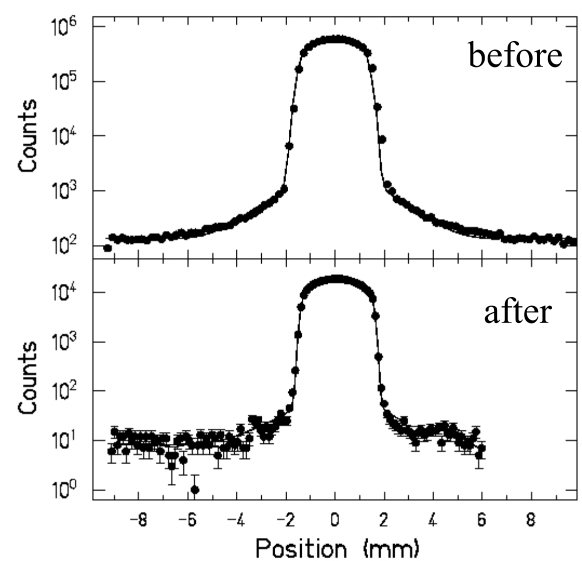

Activity scan: 51 mm heavy metal, 0.125 mm slit

Experimental chamber

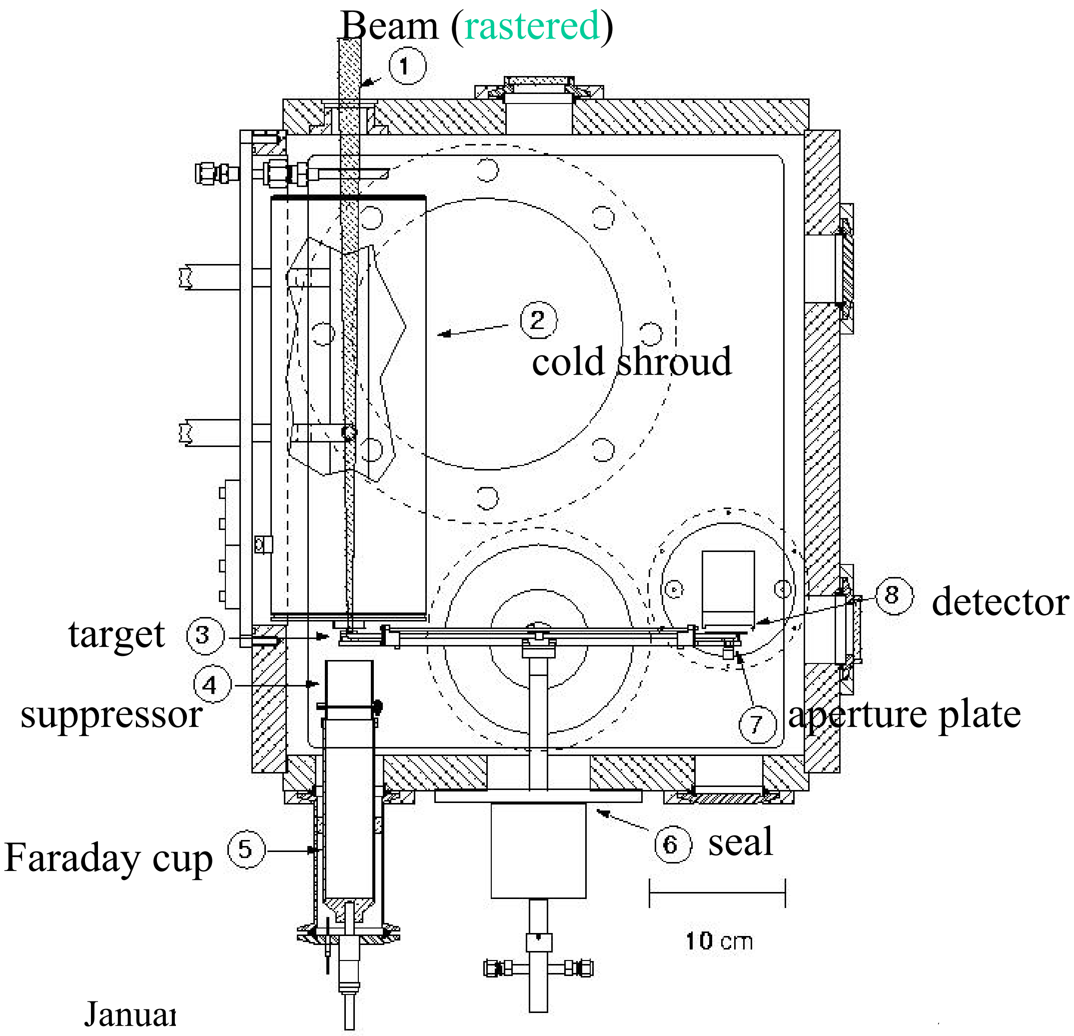

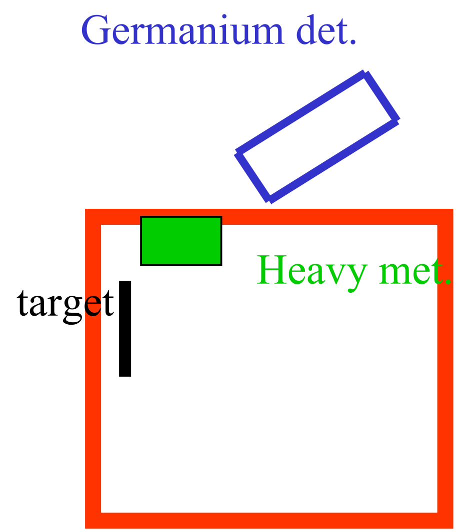

Activity measurement

Some experimental aspects

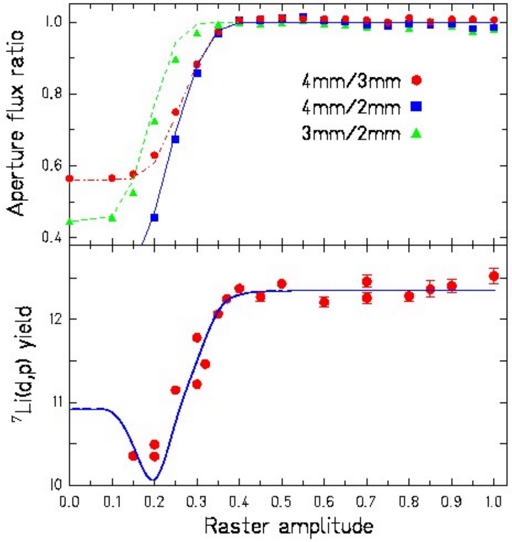

Test of raster amplitudes

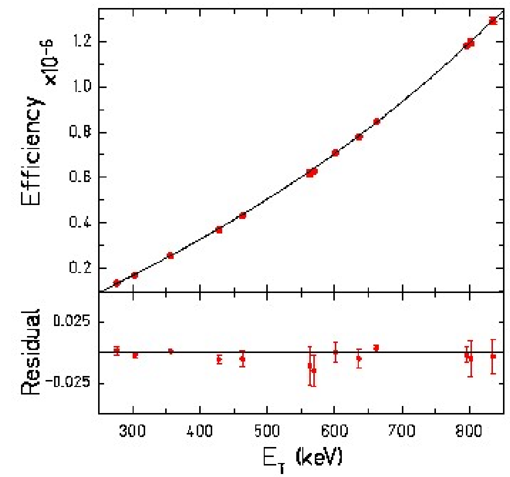

Germanium efficiency

Activity decay

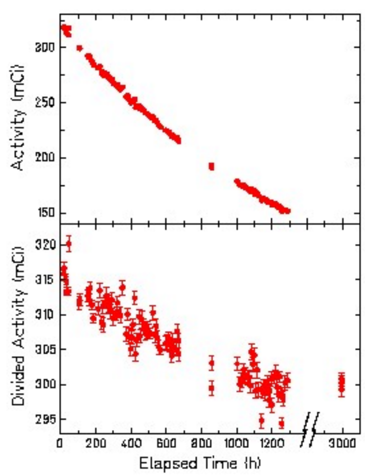

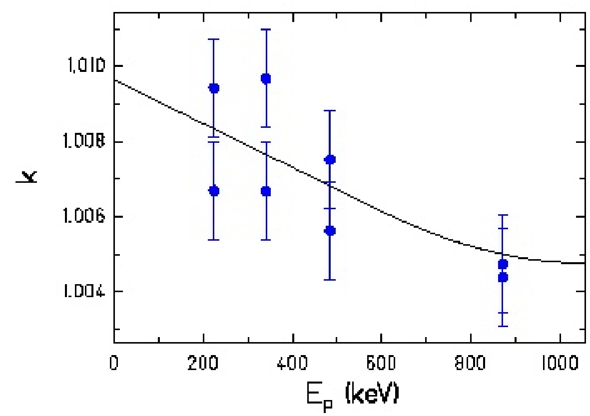

Beam energy calibration

Spectra/Backscattering

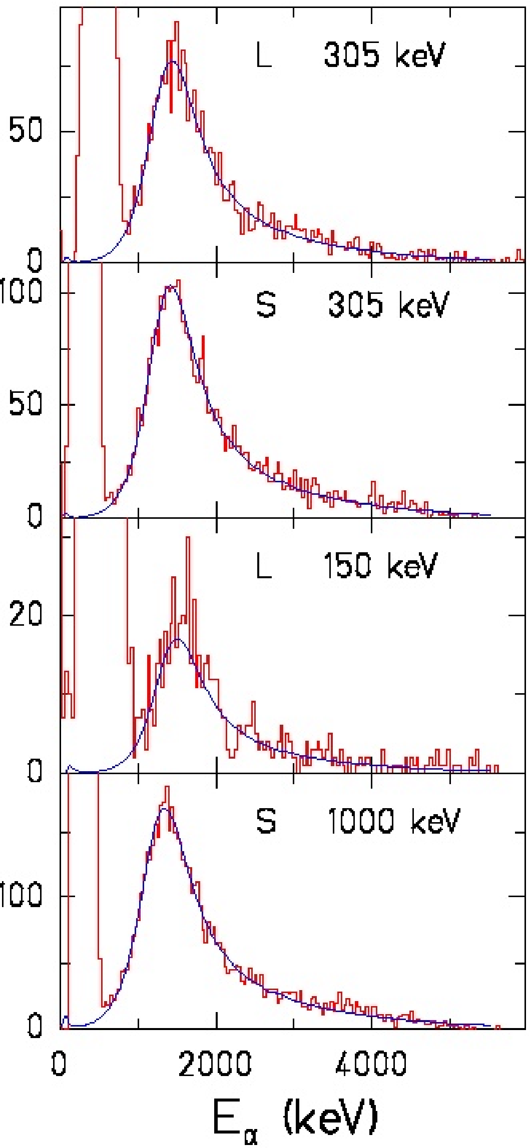

S-small detector

L-large detector

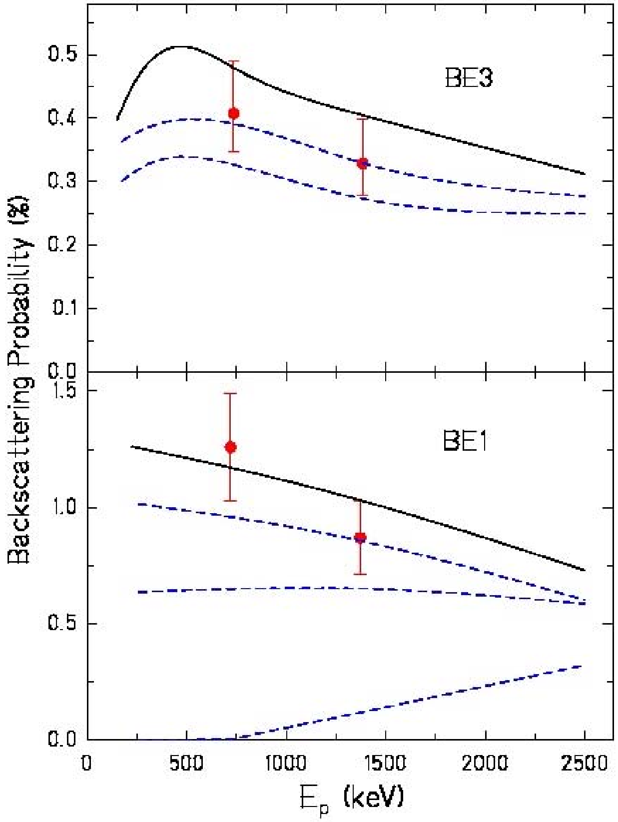

Backscattering yield

Kolka

Target profile

Scan of target by $^{7}Be(\alpha,\gamma)^{11}C$ narrow resonance.

Be3 aka Be25

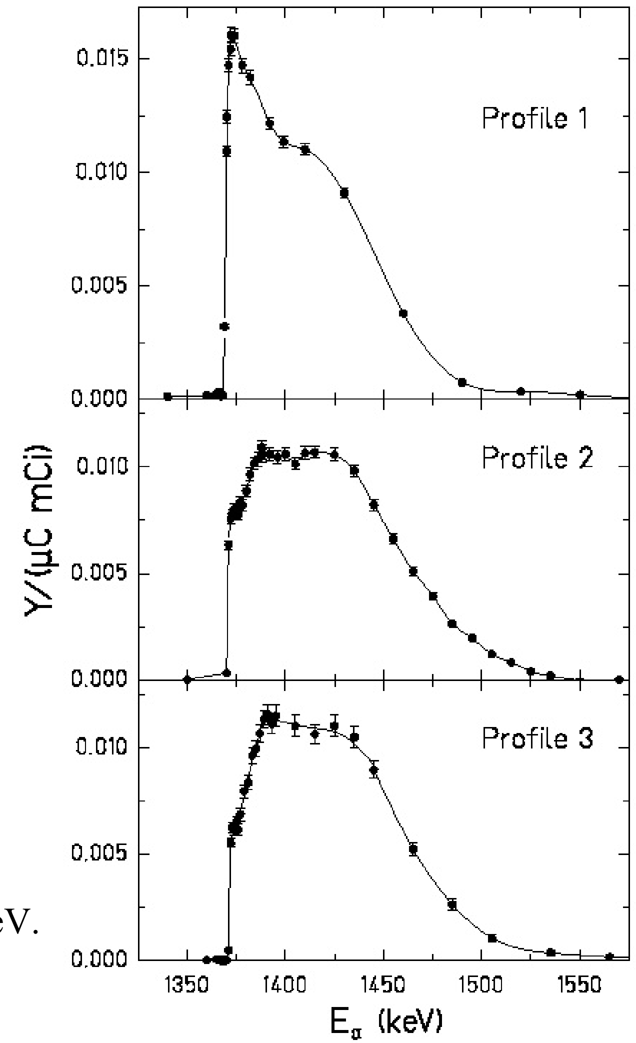

Beam energy to be shifted by 9 keV.

Cross section/S-factor

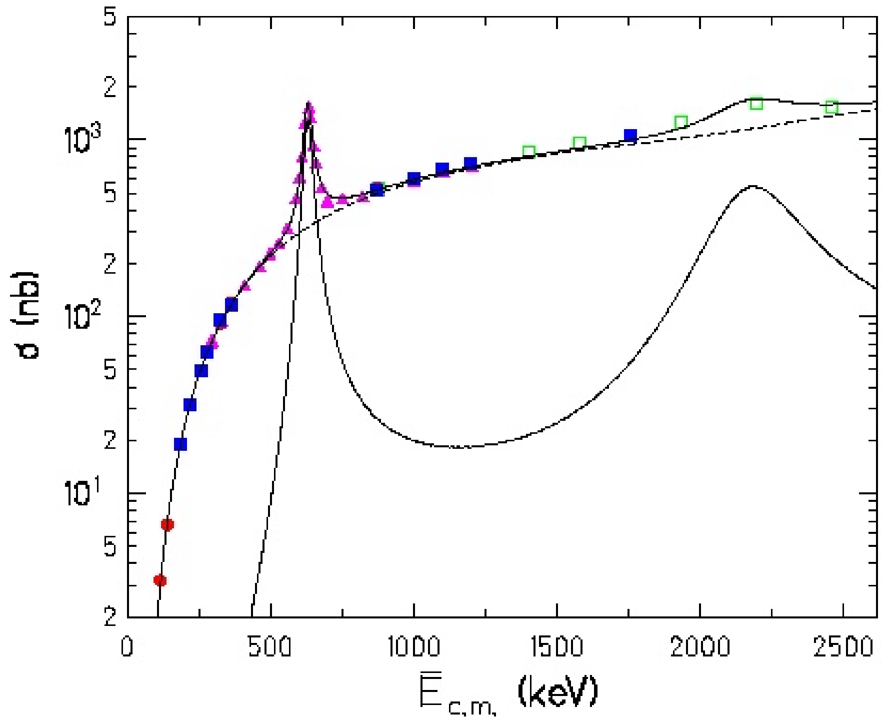

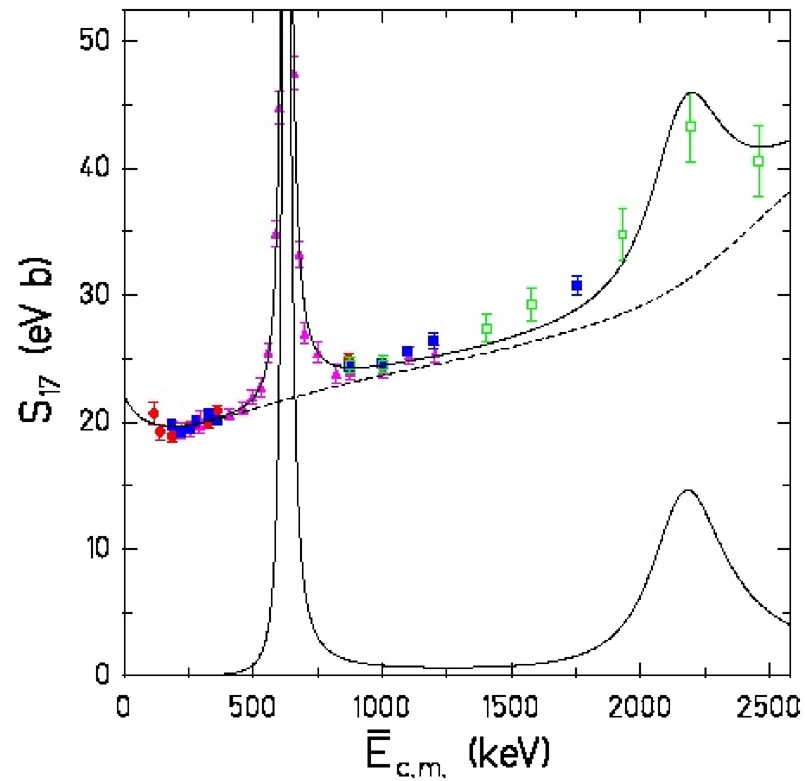

Extrapolating $^7Be(p,\gamma)^8B$

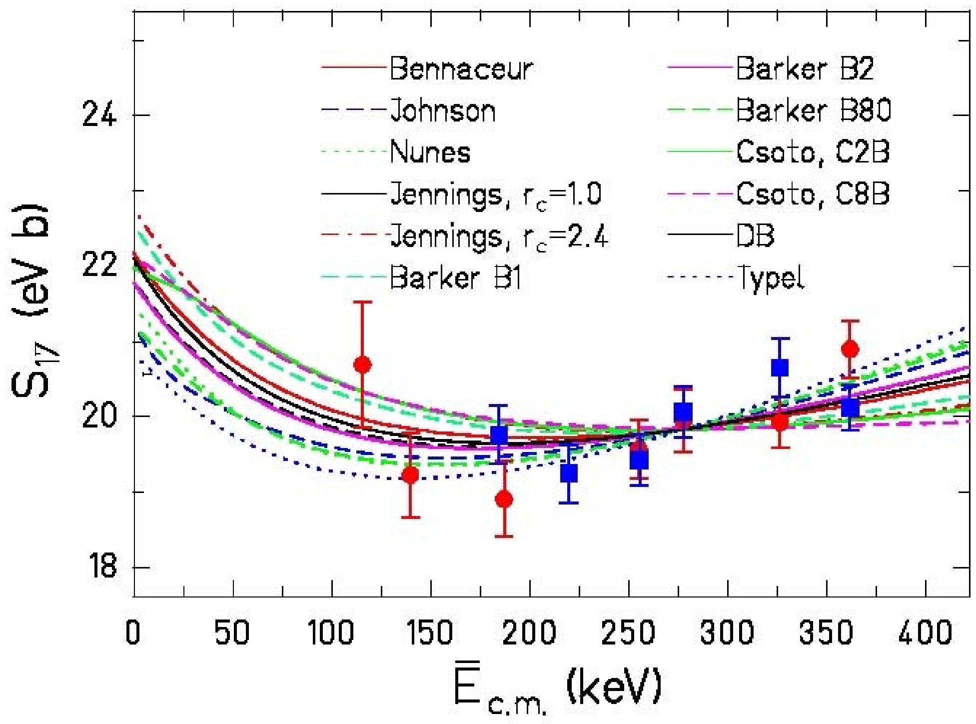

About 5% spread in extrapolation.

Phase shifts in $^7Be(p,p)^7Be$

From a paper in press by P. Descouvement: **"We suggest that reducing the current uncertainty on the experimental scattering length would significantly reduce the error bar on $S_{17}(0)$. "**

P. Descouvement finds a clearly visible phase shift difference for S=1 phase shifts between potential and his cluster models at 1 MeV and above.

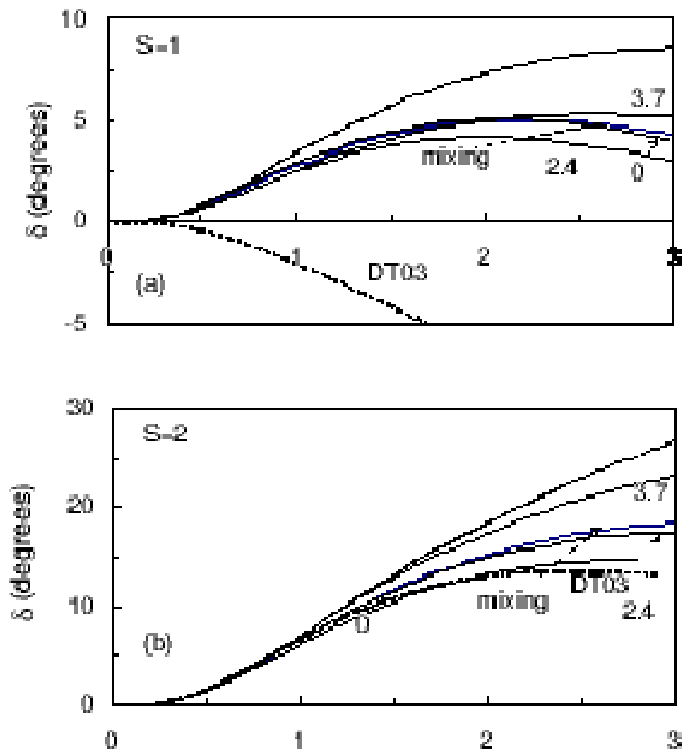

Data available for elastic scattering

Rogachev et al.

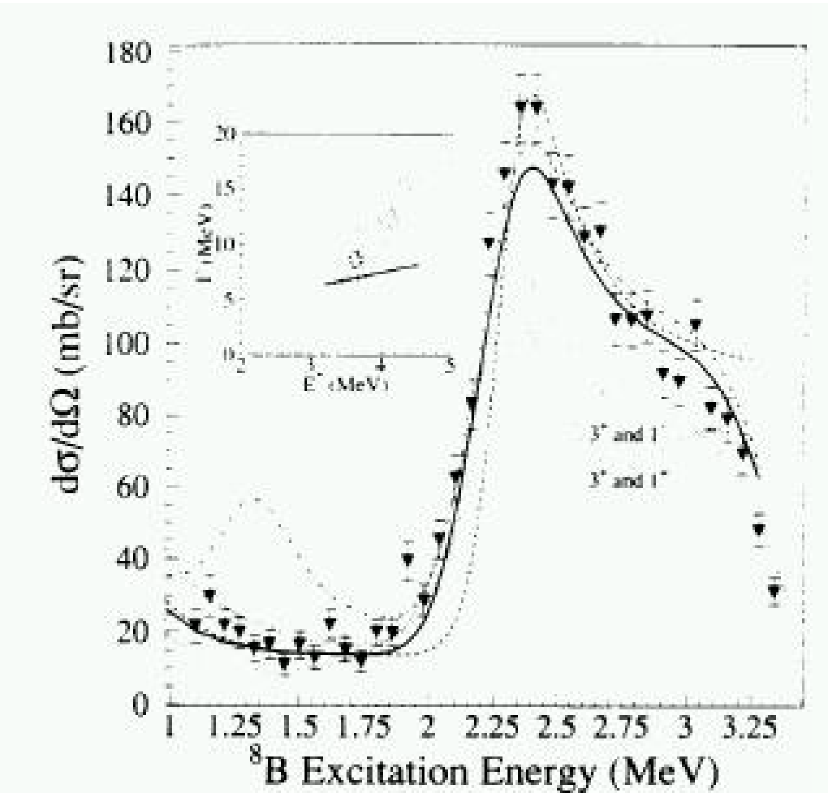

Strong 2⁻ resonance proposed

Observation of strong inelastic scattering at Oak Ridge

Cross section: 10-100 mb/sr

Angulo et al.

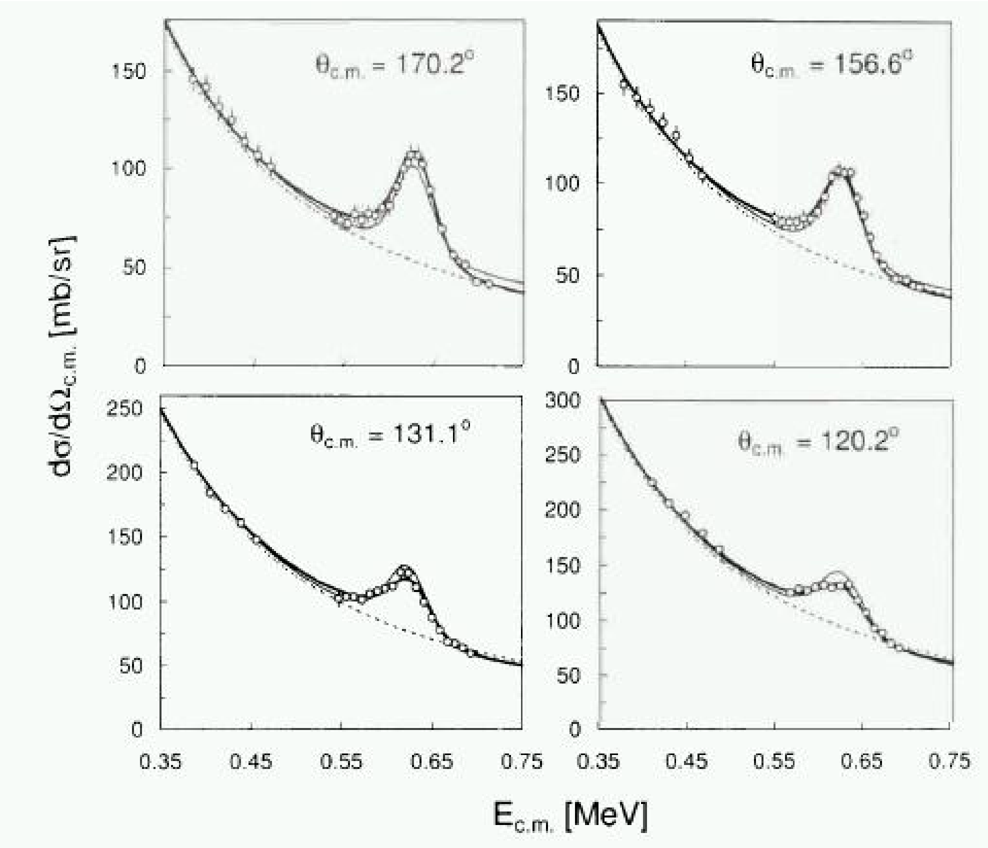

Scattering length for s=1 not compatible with ^{7}Li+n, s=2 with a 40% error. Error from uncertainties in 1^+ resonance.